FEBS 25823

FEBS Letters 513 (2002) 267–272

Solution structure of polyglutamine tracts in GST-polyglutamine fusion proteins

Laura Masino[a], Geoff Kelly[a], Kevin Leonard[b], Yvon Trottier[c], Annalisa Pastore[a,*]

[a] *National Institute for Medical Research, The Ridgeway, London NW7 1AA, UK*
[b] *EMBL, Meyerhofstrasse 1, D69117 Heidelberg, Germany*
[c] *IGBMC, CNRS, INSERM, ULP, Université de Strasbourg, Illkirch Cedex 67404, France*

Received 11 December 2001; revised 10 January 2002; accepted 15 January 2002

First published online 31 January 2002

Edited by Thomas L. James

Abstract Aggregation of expanded polyglutamine (polyQ) seems to be the cause of various genetic neurodegenerative diseases. Relatively little is known as yet about the polyQ structure and the mechanism that induces aggregation. We have characterised the solution structure of polyQ in a proteic context using a model system based on glutathione *S*-transferase fusion proteins. A wide range of biophysical techniques was applied. For the first time, nuclear magnetic resonance was used to observe directly and selectively the conformation of polyQ in the pathological range. We demonstrate that, in solution, polyQs are in a random coil conformation. However, under destabilising conditions, their aggregation behaviour is determined by the polyQ length.

Key words: Aggregation; Glutathione *S*-transferase; Huntington; Polyglutamine; Structure

1. Introduction

At present nine neurodegenerative diseases, including Huntington's disease (HD) and several forms of spinocerebellar ataxia (SCA), have been shown to be caused by anomalous expansion in their genes of CAG trinucleotide repeats, that code for polyglutamine (polyQ) tracts [1]. Except for the polyQ region, the related proteins have no sequence homology, harbour the glutamine (Q) stretch at different positions, have different subcellular localisation and, when known, different functions [2]. The length of the Q repeats determines the age of onset and the severity of the disease. In all disorders, except for SCA6, the repeats of unaffected individuals have approximately 6–35 Qs, whereas expansions ranging between 36 and 55 Qs can result in disease onset in mid-life, and expansions of 70 and above cause the juvenile form of the disease [3]. Another characteristic shared by most polyQ diseases is the accumulation of insoluble aggregates in the nucleus of a specific subset of neuronal cells [1]. The aggregates, termed neuronal intranuclear inclusions, contain the expanded protein and are thought to be a direct cause of neurodegeneration, eventually inducing cell death. A gain-of-function mechanism has been proposed, in which polyQ expansions confer a new toxic property on the mutated proteins by promoting its misfolding and aggregation.

Detailed information about the structural properties of polyQs is therefore essential to understand the causes of pathogenesis. However, relatively little is known as yet about the structure of the polyQ proteins. Studies performed with a fragment of huntingtin (exon 1) have shown that aggregation of polyQ stretches in vitro is self-driven and depends on protein concentration and repeat-length, showing good correlation with the pathogenic threshold [4,5]. This observation suggested that the formation of aggregates could be induced by a conformational change in the mutated protein, triggered by the polyQ expansion. Perutz et al. have suggested an elegant model in which shorter polyQ repeats have a random coil conformation, whereas longer repeats form β-hairpin or β-strand structures that promote aggregation through the formation of intermolecular polar zippers ([6] and references therein). Other works have either supported the hypothesis that polyQ stretches are in a β-sheet structure [7], or have proposed a random coil conformation for Q repeats of moderate length (9–17 residues) [8]. Recently, it was suggested that the structure of polyQ sequences of different lengths, both below and above the disease threshold, is a random coil [9].

However, these studies have been performed using protein fragments or isolated polyQ peptides, rather than full-length proteins, and thus do not take into account the possible effects of the protein context on the physical properties of the polyQ stretches. Moreover, because of the high insolubility of pure polyQ stretches in aqueous solvents, in several studies the peptides have been flanked by charged residues, or have been studied under extreme and non-physiological conditions, such as low pH values or organic solvents [8–10]. On the other hand, the very large size of the proteins involved in polyQ diseases makes it difficult to characterise full-length proteins.

In the present work, we have structurally characterised a model system consisting of 22 and 41 Qs fused to glutathione *S*-transferase (GST). This system was previously used in cellular studies on the influence of long polyQ tracts on the expression of GST-fusion proteins in *Escherichia coli* [11], and in the recent study of ataxin-1 expanded polyQs with histidine interruptions [12]. GST-fusion proteins were also used in the extensive work on huntingtin exon 1 performed

*Corresponding author. Fax: (44)-20-8906 4477.
E-mail address: apastor@nimr.mrc.ac.uk (A. Pastore).

Abbreviations: AU, analytical ultracentrifugation; CD, circular dichroism; EM, electron microscopy; GST, glutathione *S*-transferase; GST-Q22, fusion protein containing GST and 22 glutamines; GST-Q41, fusion protein containing GST and 41 glutamines; HSQC, hetero single quantum coherence; NMR, nuclear magnetic resonance; polyQ, polyglutamine; Q, glutamine; TOCSY, total correlation spectroscopy; UV, ultraviolet

0014-5793/02/$22.00
PII: S0014-5793(02)02335-9

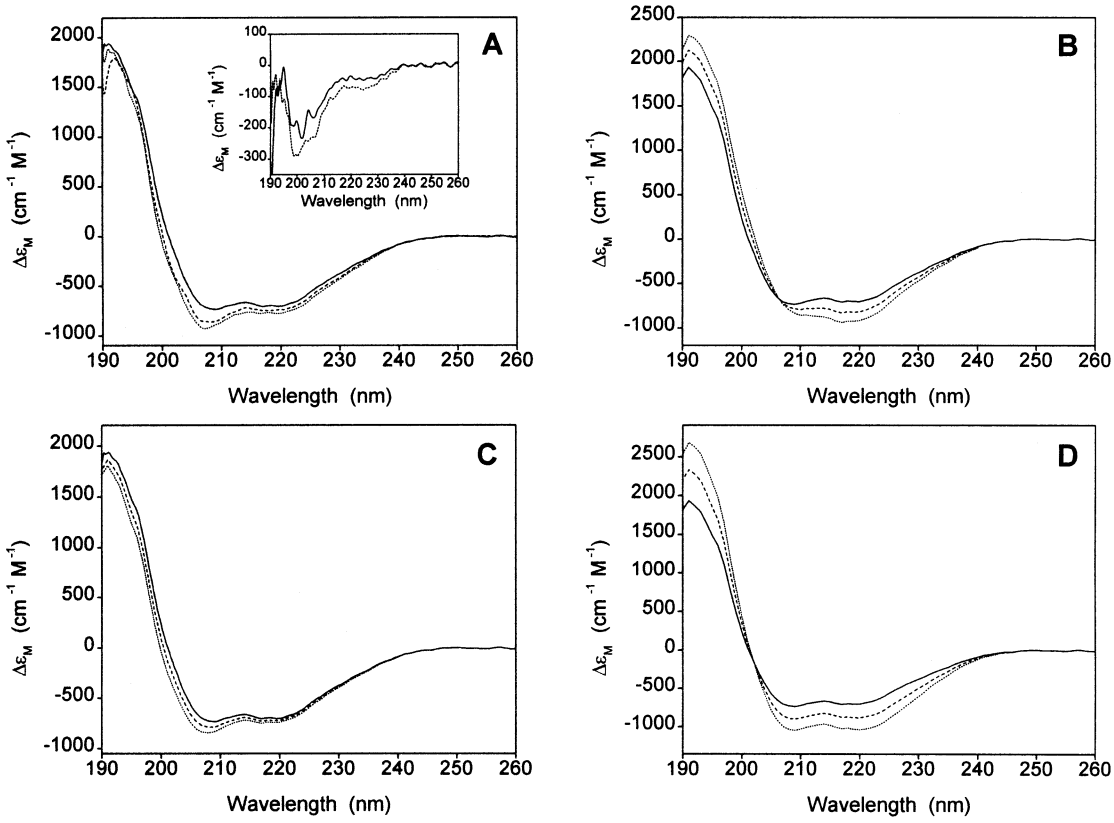

Fig. 1. A: Far-UV CD spectra of GST (—), GST-Q22 (- - -) and GST-Q41 (...). Inset: Difference spectra obtained by subtracting the spectrum of GST from those of GST-Q22 (—) and GST-Q41 (...). B,C,D: Far-UV CD spectra resulting from the addition of the spectra of 22 or 41 residues in β-sheet (B), random coil (C), or α-helix (D) to the spectrum of GST. In each panel, the curves represent GST (—), GST+22 residues (- - -) and GST+41 residues (...). The β-sheet spectra were obtained from that of synthetic polylysine in water (β-form, pH 11.1, heated at 52°C for 15 min and cooled to 22°C) [31]. The α-helix far-UV CD spectra were obtained using the spectrum of myoglobin (expressed in $\Delta\varepsilon_{mrw}$) multiplied by 22 or 41. The estimated secondary structure content of myoglobin is 80% α-helix, 5% β-turn and 14% random coil [32]. In a similar way, the random coil spectra were obtained using the spectrum of acid-denatured staphylococcal nuclease at 6°C (estimated secondary structure content: 90% random coil, 4% α-helix, 4% β-sheet and 2% β-turn) [32].

by Wanker's group [4,5,13,14]. Although in these studies GST was mostly used as a carrier from which the polyQ tracts were cleaved before being characterised, Hollenbach et al. showed that also the uncleaved GST-fusion protein self-aggregates with the same threshold observed in HD patients [14].

Here, we have selected this system to investigate the structural properties of long polyQ stretches within the context of a pure, soluble protein in native-like conditions. GST, a well characterised protein of known structure and high stability, is ideal to mimic the environment surrounding the polyQ regions in the full-length proteins. We have used a wide range of biophysical techniques to characterise the uncleaved fusion proteins. Nuclear magnetic resonance (NMR) spectroscopy has been employed for the first time to monitor directly the polyQ conformation and its time evolution, yielding structural information at the atomic level. The large size of the GST dimer (MW ~56 kDa), far from interfering with our studies, was exploited to filter selectively structural features of the polyQ tracts by NMR and to readily detect the possible formation of aggregates using low resolution techniques.

2. Materials and methods

2.1. Purification of GST-fusion proteins

The DNA sequences coding for 22 and 41 Qs were obtained from SCA2 cDNA clones [15] and were cloned into the *Bam*H1 and *Eco*R1 sites of a pGEX-4T1 plasmid vector (Amersham Pharmacia). The vector contains *Schistosoma japonicum* GST (217 residues) and a 21-residue linker at the C-terminus. The proteins were expressed in *E. coli* strain BL21 [DE3] and purified by affinity chromatography using glutathione–agarose beads (Amersham Pharmacia). Uniformly ^{15}N-labelled samples were produced by standard methods. The purity of the samples was assessed by sodium dodecyl sulphate–polyacrylamide gel electrophoresis and mass spectrometry. Protein concentrations were determined using ultraviolet (UV) absorption, with a calculated extinction coefficient at 280 nm of 40 920 for all three proteins.

All the experiments were performed with the fusion proteins GST-Q22 (containing GST and 22 Qs) and GST-Q41 (containing GST and 41 Qs), and with GST alone, as a control. Unless otherwise specified, the standard buffer used was 40 mM sodium phosphate, pH 6.5. The samples were incubated for 2 h prior to each experiment in 1–3 mM dithiothreitol to prevent cysteine oxidation.

Table 1
Q chemical shift values obtained from NMR experiments

	GST-Q22	GST-Q41	r.c.[a]
Hα	4.25 (0.02)[b]	4.23 (0.02)	4.37 ± 0.10
C′	176.3 (0.1)	176.7 (0.1)	176.3 ± 0.5
Cα	56.3 (0.1)	56.7 (0.1)	56.2 ± 0.7
Cβ	29.2 (0.1)	29.2 (0.1)	30.1 ± 0.7

[a]Random coil values from [23,24].
[b]The numbers in parentheses are standard deviations.

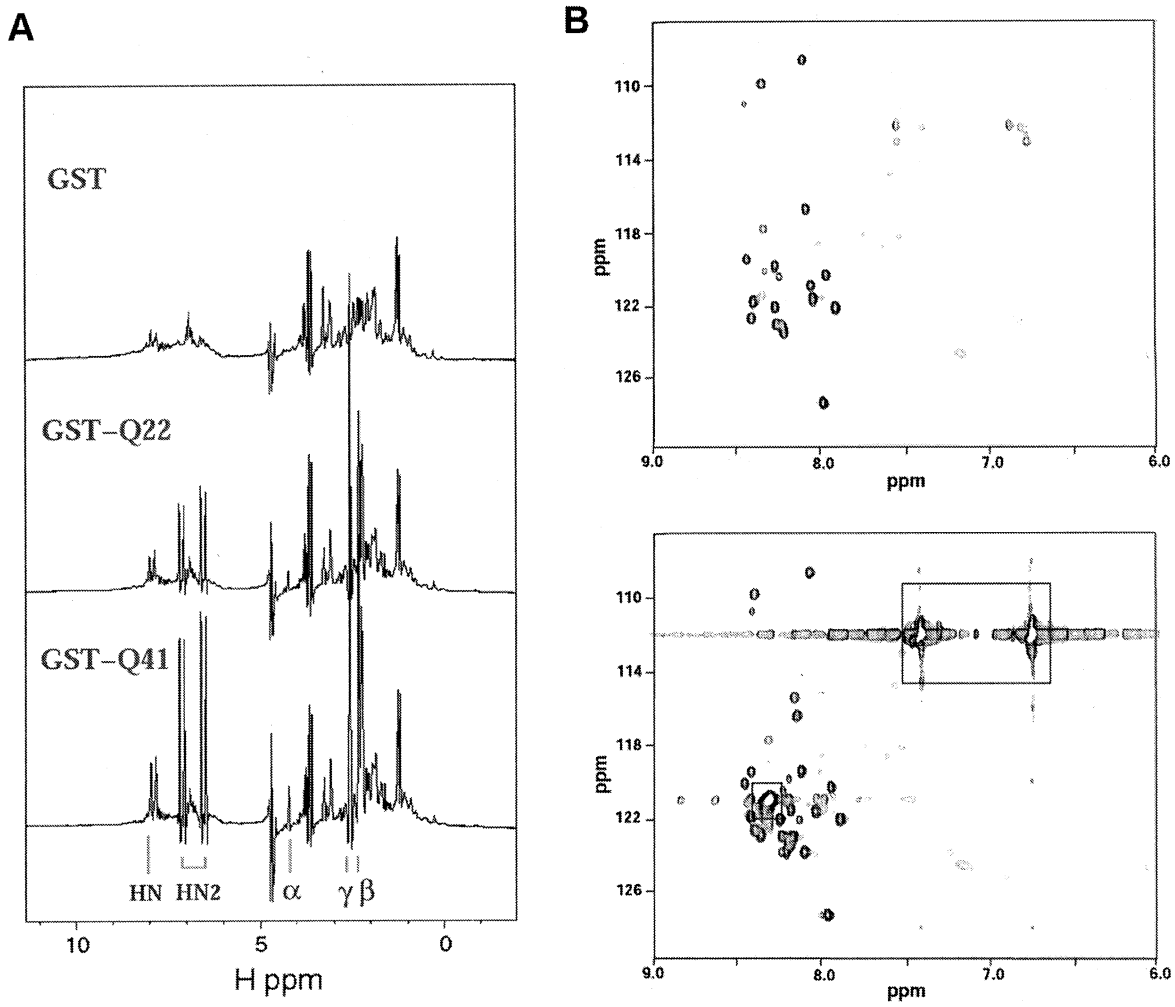

Fig. 2. NMR spectra recorded at 600 MHz and 25°C. A: 1D ^{1}H NMR spectra of GST, GST-Q22 and GST-Q41. The peak assignment of the Q residues is shown at the bottom of the figure. B: Comparison between the 2D ^{1}H–^{15}N HSQC spectra of GST (top) and GST-Q22 (bottom). The Q peaks are shown in the boxes.

2.2. Circular dichroism (CD)

Measurements were performed on a Jasco J-715 spectropolarimeter fitted with a thermostated cell holder and interfaced to a Neslab water bath. Spectra were recorded at 20°C and baseline corrected. Sample concentration was 4–6 μM and quartz cuvettes (Hellma) with pathlengths of 1 or 2 mm were used. Thermal unfolding measurements were performed by increasing temperature from 10 to 70°C at 1°C/5 min. The sample temperature was monitored using an immersed thermocouple (Comark).

2.3. Analytical ultracentrifuge

Sedimentation equilibrium experiments were performed using a Beckman XL-A ultracentrifuge equipped with UV absorption optics. Data were recorded at 8000 and 10 000 rpm, at 20, 25 and 30°C. In all data sets, the absorbance of the depleted area at a final speed of 40 000 rpm provided an experimental value for the baseline (offset). Protein concentrations were in the range of 7 to 25 μM. To determine the molecular weight of the species in solution, the data were analysed using the Origin XL-A/XL1 software (Beckman).

2.4. NMR experiments

The concentrations of the NMR samples were typically 0.4–0.6 mM. When incubated at 25°C for more than 5 h, 0.1% sodium azide, a protease inhibitor cocktail (Complete, Roche) and 0.16 mM EDTA were added to the standard buffer, to avoid proteolysis and bacterial contamination. The same NMR spectra were also recorded in the standard buffer, as a control. No differences were detected. Spectra were recorded at 25°C on Varian 500 and 600 MHz spectrometers. Two-dimensional (2D) ^{1}H total correlation spectroscopy (TOCSY) spectra were acquired at 600 MHz with a mixing time of 40 ms. 2D ^{13}C–^{1}H hetero single quantum coherence (HSQC) and HNCO spectra were recorded at natural abundance ^{13}C. 2D ^{15}N–^{1}H HSQC were recorded on ^{15}N enriched samples. Water signal suppression was achieved using the WATERGATE pulse sequence [16]. Translational diffusion coefficients were determined using the longitudinal eddy-current delay (LED) pulse sequence [17]. Series of 30 spectra were recorded by fixing τ (4 ms), Δ (155 ms) and the gradient length (4 ms), and incrementing the gradient magnitude from 0 to 65 G cm^{-1}. The method was calibrated by conducting reference diffusion measurements on aprotinin, hen egg white lysozyme and carbonic anhydrase. Solvent exchange rates were measured according to [18]. Relaxation data were recorded at 600 MHz using standard sequences [19]. The correlation time (τ_c) was calculated from the T1/T2 ratios according to the model-free approach [20]. All spectra were processed using NMRPipe [21] and analysed using XEASY [22].

2.5. Electron microscopy (EM)

Protein concentration was approximately 5 μM. The samples were negatively stained with 1% aqueous uranyl acetate and viewed with a Philips Biotwin electron microscope at 100 kV. Images were recorded on a Gatan CCD camera (1030×1300 pixels). The data were collected on three independent batches of proteins.

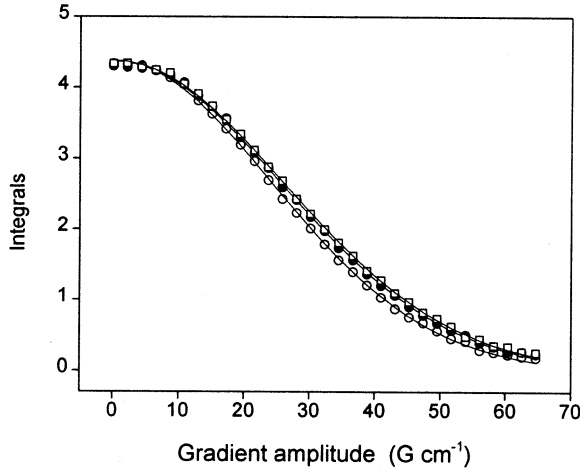

Fig. 3. NMR diffusion curves obtained for GST (○), GST-Q22 (●) and GST-Q41 (□). The solid lines are the computed best fits.

3. Results

3.1. Structural properties of the GST-fusion proteins

Two complementary spectroscopic techniques, CD and NMR, were used to determine the polyQ conformation.

The far-UV CD spectra of the three proteins are shown in Fig. 1A. The GST spectrum is typical of an α/β protein, with a predominance of the α signal. The spectra of the two fusion proteins present clear differences from the one of GST. The CD intensities for GST-Q22 and GST-Q41 are consistently more negative than that of GST, with a more pronounced difference in the 208 nm band. The difference spectra (Fig. 1A, inset), obtained by subtracting the GST spectrum from those of the fusion proteins, show that the added residues are in a random coil conformation. This observation is confirmed by the simulation in Fig. 1 (B, C and D), that shows the effects of adding far-UV CD spectra of residues in different conformations to the spectrum of GST.

Comparison of the ^{1}H NMR spectra of the three samples is shown in Fig. 2A. The 1D ^{1}H spectrum of GST is typical of a high molecular weight, folded protein. A similar envelope is observable in all three samples. The sharp resonances present only in the GST-Q22 and GST-Q41 spectra must therefore arise from the polyQ stretch. The appearance of these peaks and their intensities, which in the GST-Q41 spectrum are approximately double those in the GST-Q22 spectrum, strongly suggest that all the Qs experience a similar chemical environment. The 2D spectra are almost completely dominated by the peaks of the Q repeats which, together with a few other weaker resonances most likely rising from the residues of the peptide linker, are the only connectivities observable in the HSQC (Fig. 2B) as well as in the TOCSY spectra. While the connectivities of the bulky GST must be T2-filtered by the high molecular weight of the protein dimer, observation of resonances of the C-terminal tail directly suggests that this region is highly flexible, as confirmed also by the correlation time estimated from ^{1}H–^{15}N relaxation experiments ($\tau_c \sim 15$ ns).

Comparison of the chemical shifts of the Q resonances with tabulated values [23,24] shows that they are all consistent with a random coil conformation (see Table 1). Furthermore, water saturation experiments show that the Q backbone amide protons are highly exposed to the solvent (solvent exchange rate $\sim 7\ s^{-1}$) [25]. No differences are observed between GST-Q22 and GST-Q41. From these results we must conclude that the polyQ regions in both fusion proteins are in a highly flexible random coil conformation.

3.2. Study of stability and aggregation properties

The aggregation properties of the polyQ regions were investigated by probing freshly purified samples by analytical ultracentrifugation (AU) and by NMR diffusion experiments. The AU data are consistent with the existence of a single species in solution in each sample, with molecular weights corresponding to the dimeric form of the proteins (data not shown). The diffusion coefficients obtained from the NMR diffusion measurements (Fig. 3) are 5.0×10^{-7}, 4.5×10^{-7} and 4.3×10^{-7} $cm^2\ s^{-1}$ for GST, GST-Q22 and GST-Q41, respectively. The molecular weights calculated from these values are in good agreement with the AU results, within experimental error.

In order to determine the tendency of the proteins to aggregate over long periods of time, the samples were incubated at 25°C for 3 months and monitored by NMR over this period at 7 day intervals. No changes were observed in the NMR parameters obtained with the three samples and no differences were detected between GST-Q22 and GST-Q41. In particular, the 1D and 2D spectra recorded in each set of experiments remained superimposable. Thus, the polyQ stretches in both proteins remain in a highly flexible, random coil conformation

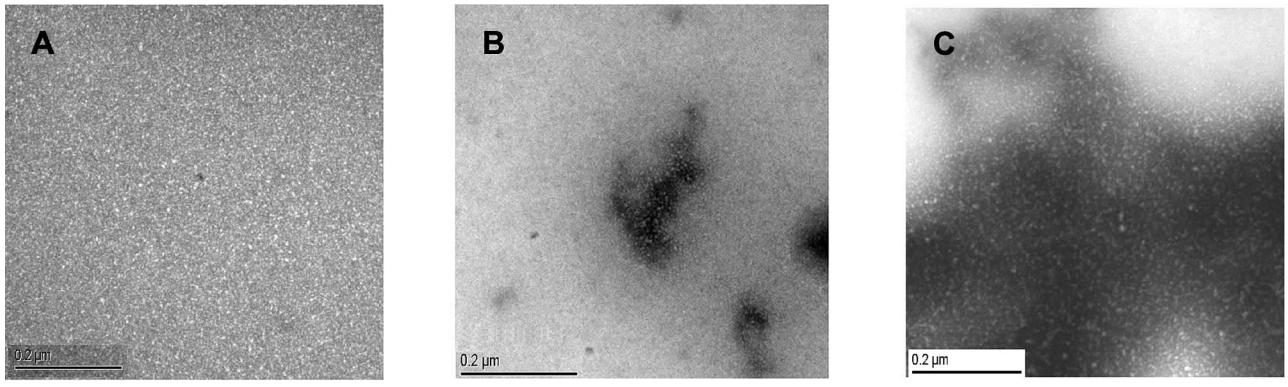

Fig. 4. Electron micrographs of negatively stained samples after incubation at 52 and 70°C. A: Native GST showing well dispersed particles; B: GST-Q22 showing some aggregation; C: GST-Q41 showing large aggregates of protein.

and the proteins do not have an appreciable tendency to aggregate and/or precipitate under the experimental conditions used.

The thermal stability of the samples was investigated by monitoring thermal unfolding using far-UV CD. In the range 10 to 50°C, the CD signal of all fusion proteins does not change, indicating that the proteins are stable in this temperature range (data not shown). However, when the temperature is raised above 50°C, all proteins start precipitating irreversibly. The similar behaviour of the fusion proteins and GST suggests that the stability properties of the fusion proteins are strongly affected by those of GST. However, qualitative differences were observed in the three samples at temperatures above 50°C. Precipitation of GST-Q41 typically started only 1/2 h after that of GST and GST-Q22, suggesting that the length of the polyQ region affects the process of aggregation.

After incubation for 1 h at 52°C and for 1/2 h at 70°C, the samples were analysed using EM in order to detect the formation of aggregates. The results show that GST-Q41 has a much greater tendency to aggregate than GST-Q22. In particular, the aggregates observed in the GST-Q41 samples are consistently much bigger in size ($\geqslant$1 μm) and more concentrated than those observed in the GST-Q22 samples. Fig. 4 shows images of GST-Q22 (B) and GST-Q41 (C) aggregates after thermal denaturation. No aggregates were observed in the GST samples (Fig. 4A).

4. Discussion

Different techniques have been applied in this work to investigate the biophysical properties of polyQ regions of different lengths using a model system based on GST. For the first time, NMR spectroscopy has permitted direct and selective observation of the conformation of polyQ stretches within a protein context, both in the non-pathological and pathological range.

We observe that, at 25°C, polyQs are highly exposed to solvent and in a random coil conformation. These results are in agreement with the work carried out by Chen et al., who showed that the conformation of polyQ peptides, irrespective of their length, is a random coil [9]. Similar results were also obtained in studies of chymotrypsin inhibitor-2 (CI2) mutants, containing insertions of four or 10 Qs. The solution and crystal structures of a dimer of these proteins showed a disordered polyQ region [26,27]. A relatively low tendency of polyQs to adopt secondary structure conformations is also supported indirectly by the observation that the longest polyQ stretch found by searching the database of known protein structures [28] contains three Qs.

It could be argued that the C-terminal position of the polyQs in the GST-fusion proteins could partially affect their structure. However, the location of the polyQ stretches varies widely within the nine proteins involved in polyQ diseases, and a few proteins, such as huntingtin, harbour the polyQ region near the N- or the C-termini [2]. The study on CI2 shows that a relatively short polyQ stretch inserted in the middle of the protein is also unstructured [26,27]. In addition, a bias due to possible interactions between the polyQ tracts and GST can be ruled out because, in the crystal structure of the GST dimer, the C-termini of each monomer point outwards so that they are exposed to solvent [29].

Our results also demonstrate that it is the protein context that influences the solubility of polyQs, which are per se insoluble. At 25°C, both GST-Q22 and GST-Q41 in fact do not aggregate over a 3 month period and their behaviour closely follows that of the highly soluble and thermodynamically stable GST. However, it is the length of the polyQ tracts that determines the tendency of the polyQ proteins to precipitate and aggregate when these processes are promoted by the environmental conditions. In our model, the behaviours of the two proteins diverge considerably above 50°C, as shown by the formation of much bigger aggregates in the case of GST-Q41 than in the case of GST-Q22, and are independent of the presence of GST. These conclusions are in good agreement with the study of Ordway et al., who showed that CAG repeats do not need to be located within one of the classic repeat disorder genes to have a neurotoxic effect [30].

In conclusion, we have shown that a number of biophysical techniques can be applied to characterise polyQ stretches directly in their protein context. Our results are consistent with a model in which polyQs in solution are random coils, and the potential conformational transitions upon aggregation are 'encoded' by the polyQ length. We are currently applying the approach used in this work to the study of full-length polyQ proteins. A detailed knowledge of the structural properties of these proteins will provide the basis for a deeper understanding of the pathogenesis of the polyQ diseases and possibly suggest new therapeutic approaches.

Acknowledgements: We would like to thank S. Howell, C. Joseph, A. Lane, S. Martin, N. Potier and C. Weber for technical support and fruitful discussion. Y.T. was funded by the Institut National de la Recherche Médicale, the Centre National de Recherche Scientifique and the Hopital Universitaire de Strasbourg (France).

References

[1] Zoghbi, H.Y. and Orr, H.T. (2000) Annu. Rev. Neurosci. 23, 217–247.
[2] Gusella, J.F. and MacDonald, M.E. (2000) Nat. Rev. Neurosci. 1, 109–115.
[3] Wanker, E.E. (2000) Biol. Chem. 381, 937–942.
[4] Scherzinger, E., Lurz, R., Turmaine, M., Mangiarini, L., Hollenbach, B., Hasenbank, R., Bates, G.P., Davies, S.W., Lehrach, H. and Wanker, E.E. (1997) Cell 90, 549–558.
[5] Scherzinger, E., Sittler, A., Schweiger, K., Heiser, V., Lurz, R., Hasenbank, R., Bates, G.P., Lehrach, H. and Wanker, E.E. (1999) Proc. Natl. Acad. Sci. USA 96, 4604–4609.
[6] Perutz, M.F. (1999) Trends Biochem. Sci. 24, 58–63.
[7] Sharma, D., Sharma, S., Pasha, S. and Brahmachari, S.K. (1999) FEBS Lett. 456, 181–185.
[8] Altschuler, E.L., Hud, N.V., Mazrimas, J.A. and Rupp, B. (1997) J. Pept. Res. 50, 73–75.
[9] Chen, S., Berthelier, V., Yang, W. and Wetzel, R. (2001) J. Mol. Biol. 311, 173–182.
[10] Perutz, M.F., Johnson, T., Suzuki, M. and Finch, J.T. (1994) Proc. Natl. Acad. Sci. USA 91, 5355–5358.
[11] Onodera, O., Roses, A.D., Tsuji, S., Vance, J.M., Strittmatter, W.J. and Burke, J.R. (1996) FEBS Lett. 399, 135–139.
[12] Calabresi, V., Guida, S., Servadio, A. and Jodice, C. (2001) Brain Res. Bull. 56, 337–342.
[13] Georgalis, Y., Starikov, E.B., Hollenbach, B., Lurz, R., Scherzinger, E., Saenger, W., Lehrach, H. and Wanker, E.E. (1998) Proc. Natl. Acad. Sci. USA 95, 6118–6121.
[14] Hollenbach, B., Scherzinger, E., Schweiger, K., Lurz, R., Lehrach, H. and Wanker, E.E. (1999) Philos. Trans. R. Soc. Lond. B 354, 991–994.
[15] Imbert, G., Saudou, F., Yvert, G., Devys, D., Trottier, Y., Garnier, J.M., Weber, C., Mandel, J.L., Cancel, G., Abbas, N., Durr, A., Didierjean, O., Stevanin, G., Agid, Y. and Brice, A. (1996) Nat. Genet. 14, 285–291.

[16] Piotto, M., Saudek, V. and Sklenar, V. (1992) J. Biomol. NMR 2, 661–665.
[17] Gibbs, S.J. and Johnson, C.S.J. (1991) J. Magn. Reson. 93, 395–402.
[18] Hwang, T.L., van Zijl, P.C. and Mori, S. (1998) J. Biomol. NMR 11, 221–226.
[19] Kay, L.E., Nicholson, L.K., Delaglio, F., Bax, A., Bax, D.A. and Bax, T. (1992) J. Magn. Reson. 97, 359–375.
[20] Lipari, G., Lipari, G. and Lipari, S. (1982) J. Am. Chem. Soc. 104, 4546–4559.
[21] Delaglio, F., Grzesiek, S., Vuister, G., Zhu, G., Pfeifer, J. and Bax, A. (1995) J. Biomol. NMR 6, 277–293.
[22] Bartels, C., Xia, T.-H., Billeter, M., Güntert, P. and Wüthrich, K. (1995) J. Biomol. NMR 5, 1–10.
[23] Wishart, D.S., Sykes, B.D. and Richards, F.M. (1992) Biochemistry 31, 1647–1651.
[24] Wishart, D.S. and Sykes, B.D. (1994) J. Biomol. NMR 4, 171–180.
[25] Spera, S., Ikura, M. and Bax, A. (1991) J. Biomol. NMR 1, 155–165.
[26] Chen, Y.W., Stott, K. and Perutz, M.F. (1999) Proc. Natl. Acad. Sci. USA 96, 1257–1261.
[27] Gordon-Smith, D.J., Carbajo, R.J., Stott, K. and Neuhaus, D. (2001) Biochem. Biophys. Res. Commun. 280, 855–860.
[28] Abola, E.E., Sussman, J.L., Prilusky, J. and Manning, N.O. (1997) Methods Enzymol. 277, 556–571.
[29] Oakley, A.J., Lo Bello, M., Ricci, G., Federici, G. and Parker, M.W. (1998) Biochemistry 37, 9912–9917.
[30] Ordway, J.M., Tallaksen-Greene, S., Gutekunst, C.A., Bernstein, E.M., Cearley, J.A., Wiener, H.W., Dure, L.S.t., Lindsey, R., Hersch, S.M., Jope, R.S., Albin, R.L. and Detloff, P.J. (1997) Cell 91, 753–763.
[31] Yang, J.T., Wu, C.S. and Martinez, H.M. (1986) Methods Enzymol. 130, 208–269.
[32] Sreerama, N., Venyaminov, S.Y. and Woody, R.W. (2000) Anal. Biochem. 287, 243–251.